NRL REPORT 3648

FR-3648

CHARGE STORAGE IN CATHODE-RAY TUBES

C. V. Parker

March 17, 1950

Approved by:

Dr. C. E. Cleeton, Head, Security Systems Branch
Dr. J. M. Miller, Superintendent, Radio Division I

NAVAL RESEARCH LABORATORY

CAPTAIN F. R. FURTH, USN, DIRECTOR
WASHINGTON, D.C.

DISTRIBUTION

BuShips	
Attn: Code 820	10
ONR	
Attn: Code 427	2
OpNav	1
Attn: Op-413	2
BuAer	
Attn: Code Aer-El-83	2
BuOrd	
Attn: Code Re4f	2
Dir., USNEL	2
Attn: Dr. R. O. Burns	2
CDR, USNOTS	
Attn: Reports Unit	2
Supt., USNPGS	1
Dir., Armed Forces Security Agency	1
OCSigO	
Attn: Ch. Eng. & Tech. Div., SIGTM-S	1
CO, SCEL	
Attn: Dir. of Eng.	2
Dir., ESL	
Attn: Mr. S. Levine	1
CG, USAF	
Attn: AFMEN	1
Wright-Patterson AFB	
Attn: CADO-D	1
Attn: BAU-CADO	1
Attn: Eng. Div., Electronics Subdiv., MCREEO-2	1
Attn: MCREEC	1
Attn: MCREEC-53	1
CO, Watson Labs., Red Bank, N. J.	
Attn: Ch. Eng. Div., ENG	1
Attn: ENR	1
CO, Air Force Cambridge Res. Lab.	
Attn: ERRS	1
Attn: Mr. C E. Ryan	1
Attn: Mr. J. V. Harrington	1
Attn: Mr. T F. Rogers	1
Dir., NBS	
Attn: CRPL	1
ANDB	
Attn: Capt. Cogswell	2
RDB	
Attn: Information Requirements Branch	2
Attn: Navy Secretary	1
Naval Res. Sec., Science Div., Library of Congress	
Attn: Mr. J. H. Heald	2

CONTENTS

ABSTRACT

The charging process in cathode-ray tubes used for static storage of information is analyzed both for a stationary spot and a linear scan, with and without redistribution of secondary electrons. Approximate equations are derived for the surface potentials and charging current as functions of time and other parameters, such as primary beam current, writing speed, and initial potentials.

PROBLEM STATUS

This is an interim report; work is continuing on the problem.

AUTHORIZATION

NRL Problem 03-06R
NR 503-060

CHARGE STORAGE IN CATHODE-RAY TUBES

INTRODUCTION

When a scanning cathode-ray beam impinges on an insulating material such as the screen of an ordinary cathode-ray tube, it leaves behind a trail of electrical charge which may be followed at a later time to discover the events which previously occurred. This phenomenon of static storage has recently found widespread application in both military and civilian fields and is therefore worthy of intensive theoretical and experimental study. The purpose of the present paper is to attempt an approximate analysis of the charging action and to deduce the effects of various parameters of the process on the output current.

The analysis may be conveniently undertaken in four well-defined steps as follows:

(I) Spot charging without redistribution.
(II) Scanning without redistribution.
(III) Spot charging with redistribution.
(IV) Scanning with redistribution.

By redistribution is meant here the return of secondary electrons to regions of the insulating surface other than the region directly under the electron beam from which the secondaries arose. The division of the analysis into the four parts given above arises naturally from the increasing complexity of the phenomena. Parts I and II apply approximately to cathode-ray tubes containing grids close to the insulating surface, such as the Haeff Memory Tube[1] or the RCA barrier-grid tube,[2] while parts III and IV apply to ordinary cathode-ray tubes used for storage purposes such as described by McConnell,[3] and Williams and Kilburn.[4] An analysis[5] of a barrier-grid tube with "backing-plate" modulation has recently been published; the results are similar to some of those to be described in Part II of this paper but differ in detail because of the approach.

---

[1] *Haeff, A. V., "A Memory Tube," Electronics, Vol. 20, pp. 80-83, Sept. 1947*

[2] *Jensen, A. S., Smith, J. P., Mesner, M. H., and Flory, L. E., "Barrier Grid Storage Tube and Its Operation," RCA Review, Vol. IX, No. 1, pp. 112-135, March 1948*

[3] *McConnell, R. A., "Video Storage by Secondary Emission from Simple Mosaics," Proc. I.R.E., Vol. 35, p. 1258-1264, Nov. 1947*

[4] *Williams, F. C., and Kilburn, T., "A Storage System for Use with Binary-Digital Computing Machines," Journal I.E.E., Part IIIA, Vol. 96, p. 81-100, March 1949*

[5] *Harrington, J. V., "Storage of Small Signals on a Dielectric Surface," Cambridge Field Station Report No. E5045, March 1949*

The generalized storage tube to be considered will consist of an evacuated envelope containing at least the following parts: An electron gun, deflecting plates, a collector electrode, and a target electrode made up of an insulating material backed by a conducting plate. The collector electrode will normally be assumed to be at the highest potential of any electrode in the tube (usually ground potential), with the cathode sufficiently negative to the collector to make the secondary emission ratio δ greater than unity for the insulating material being used for the target. The output terminal will be taken as the conducting plate of the target electrode, which is assumed connected to the collector through a suitable output resistor. In order to simplify the mathematical analysis, various assumptions and simplifications will subsequently be made; but it may be stated at the outset that the following effects will be neglected throughout, either because of their minor importance or because their effects are independent of those to be discussed, and hence may be superposed later:

(a) Leakage across or through the target material,
(b) The "cloud" effect of Williams and Kilburn,[6]
(c) Nonuniformities of target surface,
(d) Transit times of secondary electrons, both before and after emission,
(e) Space-charge effects.

PART I

SPOT CHARGING WITHOUT REDISTRIBUTION

It is by this time well-known that current flows in the output resistor when the primary beam is first turned on, due to the charging current to the capacitance formed by the spot under the electron beam with the back plate of the target electrode. A secondary current consisting of δ secondaries for each primary is emitted from the spot, which will temporarily be assumed to be initially at collector potential. These secondaries will be carried by their initial kinetic energy to the collector. However, since we have assumed an accelerating potential for the primary beam such that δ is greater than unity, the spot charges positively due to the loss in electrons, and the charge density continues to increase with time. Those secondaries with the lowest kinetic energy of emission are pulled back to the spot by its positive charge, and the apparent secondary emission ratio is reduced. Secondaries of higher and higher energy are pulled back as the spot charges until eventually a condition of equilibrium is reached in which the apparent secondary emission ratio is unity. In Figure 1, the number, N, of secondary electrons of initial energy between E and E + dE electron volts emitted per second is assumed to vary with E according to a function f(E). The total area under the curve represents the total number of electrons emitted per second, which may be taken for our purposes as proportional to δI_0 where I_0 is the beam current. The area not cross-hatched in Figure 1 represents the fraction of the total number of secondary electrons which return to the spot per second after the equilibrium potential has been reached. The cross-hatched area then represents the current I_0 which flows to the collector. Thus the following equations may be written:

$$\delta I_0 = \int_0^{\infty} f(E)\,dE, \tag{1}$$

$$I_0 = \int_{E_e}^{\infty} f(E)\,dE, \tag{2}$$

---

[6] *Williams, F. C., and Kilburn, T., op. cit.*

$$(\delta-1)I_0 = \int_0^{E_e} f(E)\,dE. \quad (3)$$

The potential of the spot V with respect to the collector (which is assumed at ground potential) may be related to the energy E of the secondary electrons by the following considerations. In order that a secondary electron may escape from the spot and reach the collector, it must possess at least as much kinetic energy initially as its potential energy in the field of the spot just before reaching the collector. If the penetration of the field of the accelerating and deflecting electrodes into the region of interest is negligible, this potential energy in electron volts is simply the potential of the spot. Thus, in this case of no redistribution, the abscissa E of Figure 1 may be identified as the potential of the spot V. Hence, the fractional part of the secondary current δI_0 which returns to the spot may be defined as $S\delta I_0$ given by

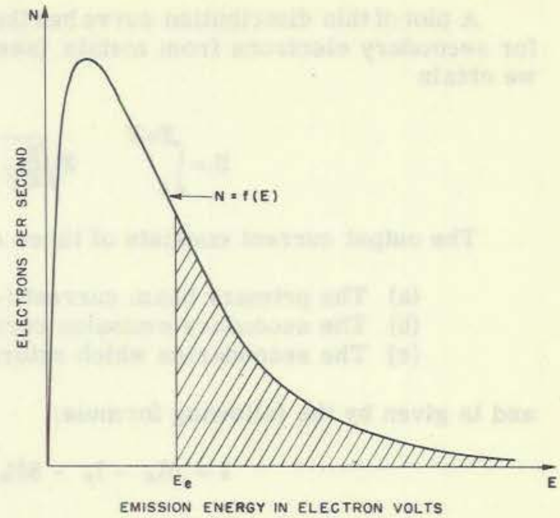

Figure 1 - Energy distribution curve for secondary electrons

$$S\delta I_0 = \int_0^{E=V} f(E)\,dE \quad (4)$$

from which S is defined as

$$S = \frac{\int_0^{E=V} f(E)\,dE}{\int_0^{\infty} f(E)\,dE}. \quad (5)$$

From this definition it is clear that if f(E) passes through the origin, S is zero when V is zero. In the case of thermionic emission, the energy distribution of escaping electrons is Maxwellian. In particular,[7] the Z-directed energy distribution (the Z axis is taken perpendicular to the surface from which the electrons are emitted) is given by

$$\frac{d(L_E/L)}{dr} = 2re^{-r^2} \quad (6)$$

where

$\frac{L_E}{L}$ = rate of arrival of particles with energies due to Z-directed motion greater than E divided by the rate of arrival of particles with all energies

$$r = \sqrt{\frac{E}{E_T}} \quad (7)$$

E_T = Average energy due to Z-directed motion.

---

[7] *Dow, W. G., "Fundamentals of Engineering Electronics," John Wiley & Sons, 1937, p. 237*

A plot of this distribution curve has the same general shape[8] as that found experimentally for secondary electrons from metals (see Figure 1). Hence, taking $f(E)\,dE = [d(L_E)/dr]\,dr$, we obtain

$$S = \int_0^{E=V} 2\sqrt{\frac{E}{E_T}}\; e^{-E/E_T}\; d\left(\sqrt{\frac{E}{E_T}}\right) = 1 - e^{-\frac{V}{E_T}}. \quad (8)$$

The output current consists of three components:

(a) The primary beam current $(-I_0)$,
(b) The secondary emission current (δI_0), and
(c) The secondaries which return to the surface after emission $(-S\delta I_0)$,

and is given by the following formula:

$$I = \delta I_0 - I_0 - S\delta I_0 = C\frac{dV}{dt} \quad (9)$$

where:

C is the capacitance between the spot and the conducting back plate,
dV/dt is the time rate of change of the effective potential of the spot.

Using the value of S from equation (8), the following differential equation is obtained:

$$\frac{dV}{dt} - \frac{\delta I_0}{C}\, e^{-V/E_T} + \frac{I_0}{C} = 0 \quad (10)$$

If we specify that the initial potential of the spot is V_i, the solution of this differential equation is

$$V = E_T \ln\left[\delta + \left(e^{V_i/E_T} - \delta\right) e^{-\gamma t}\right] \quad (11)$$

where

$$\gamma = \frac{I_0}{C\,E_T}. \quad (12)$$

Note that at very large values of time, the potential approaches

$$V_e = E_T \ln \delta. \quad (13)$$

The output current is

$$\frac{I}{I_0} = \frac{C}{I_0}\frac{dV}{dt} = \delta e^{-V/E_T} - 1 \quad (14)$$

as a function of voltage and

$$\frac{I}{I_0} = \frac{\left(\delta - e^{V_i/E_T}\right) e^{-\gamma t}}{\delta - \left(\delta - e^{V_i/E_T}\right) e^{-\gamma t}} \quad (15)$$

---

[8] *Salow, H., "Die Sekundärelektronenemission," F.T.Z., Heft 6, p. 161-165, Juni 1949*

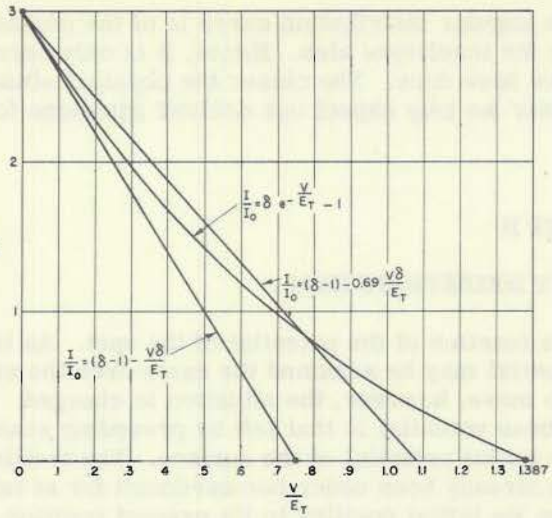

Figure 2 - Output current vs. V/E_T *for* $S = e^{-V/E_T}$ *and for* $S = V/E_T$, $\delta = 4$
Stationary spot with no redistribution

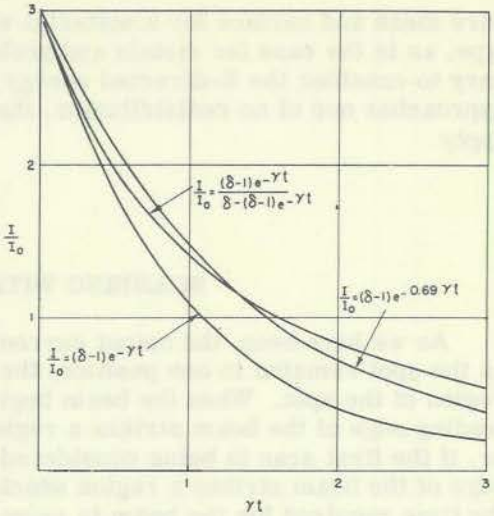

Figure 3 - Output current vs. γt *for* $S = e^{-V/E_T}$ *and for* $S = V/E_T$, $\delta = 4$
Stationary spot with no redistribution

as a function of time. In Figures 2 and 3 the output current is plotted versus potential of the spot and time, respectively, assuming $\delta = 4$, $V_i = 0$. It will be observed that the curves may be approximated to a fair degree of accuracy by a linear function of potential and a simple exponential function of time. These approximate results would be obtained if the exponential in equation (8) were expanded in a power series and only the first two terms retained; i.e., $e^{-x} \cong 1 - x$. In order to obtain better agreement between the more exact expressions and their simpler approximations over a wide range of the independent variables, a constant factor m may be introduced so that $S = mV/E_T$. ($m = 0.69$ in the appropriate curves of Figures 2 and 3.) This approximation will be useful in the more complicated cases to be considered in Parts III and IV.

The physical situation makes it clear that the maximum output current obtainable is $(\delta - 1)\,I_0$ and the minimum current is $-I_0$. Thus, S lies in the range between zero and plus one inclusive and, since V/E_T is positive, m must be positive also. If the potential V is made negative, either by positive bias on the collector or by the deposition of negative charge on the dielectric surface, the derived equations do not apply since the output current can be no greater than $(\delta - 1)I_0$. However, if V is made positive by negative bias on the collector or otherwise, the equations correctly predict the approach to the constant value $-I_0$ with increase in V. In either case the charging process, if allowed to continue long enough, automatically brings the surface to zero potential with respect to the collector after which the derived equations apply.

So far nothing has been said about the effect of radially directed energies of the secondary electrons. It may safely be assumed that the distribution is symmetrical about the Z axis and that the largest number of secondaries are emitted in the Z direction. The assumed condition of no redistribution may be approximated in the practical case by a wire mesh whose spacing from the insulating surface is very small compared with the spot size. With that geometrical situation, only a very small fraction of those secondary electrons whose Z-directed energy is insufficient to permit them to reach or pass through the wire mesh but whose radially directed energy is large will fall outside the boundaries of the spot. The number of such electrons approaches zero with decreasing spacing between wire mesh and surface for a material whose angular distribution curve is of the cosine type, as is the case for metals and probably for insulators also. Hence, it is only necessary to consider the Z-directed energy as we have done. The closer the physical situation approaches one of no redistribution, the closer we may expect our derived equations to apply.

PART II

SCANNING WITHOUT REDISTRIBUTION

As we have seen, the output current is a function of the potential of the spot. As long as the spot remains in one position, the potential may be assumed the same over the entire region of the spot. When the beam begins to move, however, the situation is changed. The leading edge of the beam strikes a region whose potential is that left by preceding scans or, if the first scan is being considered, the initial potential of the surface. The trailing edge of the beam strikes a region which has already been under bombardment for at least the time required for the beam to move from its initial position to its present position, and the parts of the beam between the leading and trailing edges strike regions at intermediate potentials. In order to determine the output current, then, it is necessary to sum all the current contributions of these regions or, since the charge distribution may be assumed continuous, to integrate over the area of the spot.

Two assumptions will now be made for the sake of simplicity in further analysis:

(a) The beam (and hence the spot) is rectangular in cross-section, and is of width a in the direction of scan and height b perpendicular to the direction of scan.

(b) The scanning motion is linear; i.e., the writing speed $W = dx/dt$ is constant.

The assumption will also be made that the previously derived equation for the potential may be applied to each incremental area b dx of the spot with the functional dependence of S upon the potential of the incremental area the same as in the case of the stationary spot. Defining the primary beam current denisty as $J_0 = I_0/ab$ and the capacitance per unit area as C/ab, it follows as in Equation (9) that

$$dI = \delta J_0 \left(1 - \frac{1}{\delta} - S\right) b\, dx = \frac{C}{ab} \cdot b\, dx \cdot \frac{dV}{dt} \qquad (16)$$

as the contribution of current from area b dx. The total current is

$$I = \int_0^a \frac{C}{a} \frac{dV}{dt}\, dx. \qquad (17)$$

When the beam is first turned on and the scan begins, a transient current flows to charge the entire area of the spot. However, after the time required for the spot to move its own width, a steady-state condition is reached in which the total current is constant. Because of its simplicity and practical importance, the steady state will be considered first. Since $W = dx/dt$, the integral may be evaluated by changing the variable of integration from x to t with the limits of integration t = 0 when x = 0 and t = a/W when x = a. Thus

$$I = \frac{C}{a}\int_0^{\frac{a}{W}} \frac{dV}{dt} W dt = \frac{WC}{a}\left[V\left(t = \frac{a}{W}\right) - V_i\right]. \qquad (18)$$

Using the value of V from equation (11):

$$I = \frac{WC}{a}\left\{E_T \ln\left[\delta + \left(e^{V_i/E_T} - \delta\right)e^{-\gamma a/W}\right] - V_i\right\} \qquad (19)$$

$$\frac{I}{I_0} = \frac{W}{\gamma a}\ln\left[\delta + \left(e^{V_i/E_T} - \delta\right)e^{-\gamma a/W}\right] - \frac{WCV_i}{aI_0} \qquad (20)$$

Figure 4 shows I/I_0 and V/E_T plotted as functions of $\gamma a/W = I_0 a/WCE_T$ for the special case of $V_i = 0$, $\delta = 4$. With other parameters held constant, the V/E_T curve also indicates the way in which the output current in the steady state varies with primary beam current, since from equation (18) I is linear in V.

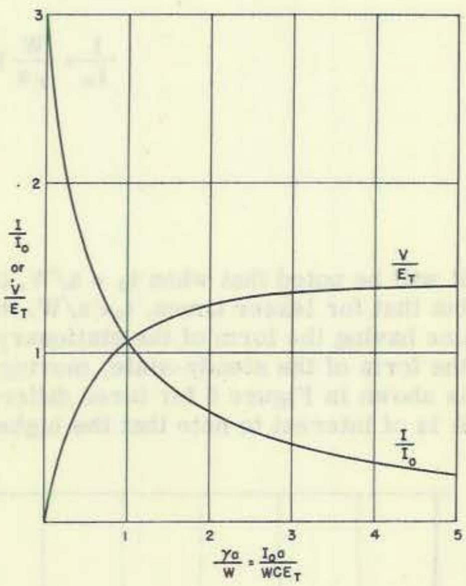

Figure 4 - Steady-state output current and potential vs. $\gamma a/W$ for δ = 4, V_i = 0. Scanning beam with no redistribution

In the transient state, the integration over x must be carried out with t held fixed. The rate of change of potential with respect to time must therefore be expressed as a function of x. The appropriate relationship may be obtained from the following considerations. Referring to Figure 5, the initial and present positions of the spot are indicated by the dotted and solid lines, respectively. The points between A and B have been charging for the full time t_0 since the beam was turned on and began its motion from left to right, and points between O and A have been charging for varying lengths of time. Thus, point O has been charging for zero time, and point x has been charging for a time $t = x/W$. Hence, the time rate of change of potential is the same for all points between A and B but varies between x = 0 and $x = Wt_0$ (point A). Thus, the integration must be carried out in two parts

$$I = \frac{C}{a}\int_{x=0}^{x=Wt_0} \frac{dV}{dt}(x)dx + \frac{C}{a}\int_{x=Wt_0}^{x=a} \frac{dV}{dt}(t_0)\,dx. \quad (21)$$

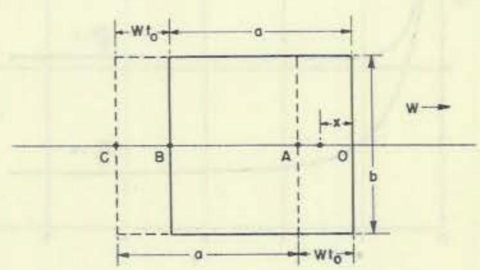

Figure 5 - Initial and present positions of spot for scanning beam transient analysis, no redistribution

In the first integral, time t_0 in the equation for dV/dt (which is equation (15) multiplied by I_0/C) may be replaced by $t_0 = x/W$ and the integration carried out with respect to x or, as was done for the steady-state case, dV/dt may be left a function of t_0 and dx replaced by Wdt_0. In either case, we obtain for the first integral

$$\frac{WC}{a}\left\{E_t \ln\left[\delta + \left(e^{V_i/E_T} - \delta\right) e^{-\gamma t_0}\right] - V_i\right\}. \qquad (22)$$

In the second integral, dV/dt is independent of x and hence may be taken outside the integral sign. Thus we obtain

$$\frac{I_0\left(\delta - e^{V_i/E_T}\right) e^{-\gamma t_0}\left(1 - \frac{Wt_0}{a}\right)}{\delta - \left(\delta - e^{V_i/E_T}\right) e^{-\gamma t_0}}$$

and

$$\frac{I}{I_0} = \frac{W}{\gamma a} \ln\left\{\delta + \left(e^{V_i/E_T} - \delta\right) e^{-\gamma t_0}\right\} - \frac{WC\,V_i}{a\,I_0} + \frac{\left(\delta - e^{V_i/E_T}\right) e^{-\gamma t_0}\left(1 - \frac{Wt_0}{a}\right)}{\delta - \left(\delta - e^{V_i/E_T}\right) e^{-\gamma t_0}}. \qquad (23)$$

It will be noted that when $t_0 = a/W$, this expression reduces to that for the steady state, but that for lesser times, $t_0 < a/W$, the output current consists of the sum of two functions, one having the form of the stationary spot current multiplied by $(1 - Wt_0/a)$ and the other the form of the steady-state, moving-beam current. The form of the resultant current is shown in Figure 6 for three different values of $\gamma a/W$ in the special case of $\delta = 4$, $V_i = 0$. It is of interest to note that the higher the writing speed the greater the final output current and also the sharper the "spike" at the beginning of the signal. The initial current is independent of writing speed and is directly proportional to the beam current.

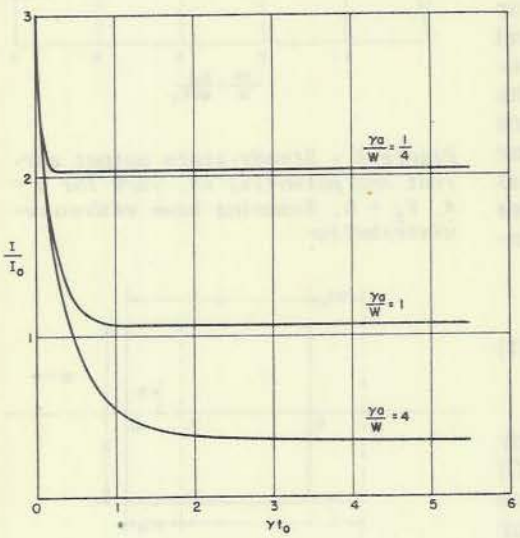

Figure 6 - Transient output current vs. γt_0 for $\delta = 4$, $V_i = 0$. Scanning beam with no redistribution

Figure 7 and 8 are photographs of the experimental output current obtained on an early model of the Haeff Memory Tube.[9] All parameters except writing speed were held constant during these photographs. The beam current was turned on for twenty-microsecond intervals in a sequence of three times on followed by one off period, during which the "hold gun" was pulsed on to provide erasure. Thus the photographs show the large output on the first scan (after erasure) which charges the surface to equilibrium except at the beginning and end of the on periods. Hence, transient outputs appear at these points on subsequent on times. The off times show in these photographs as mere closures of the

[9] *Haeff, A. V., op. cit.*

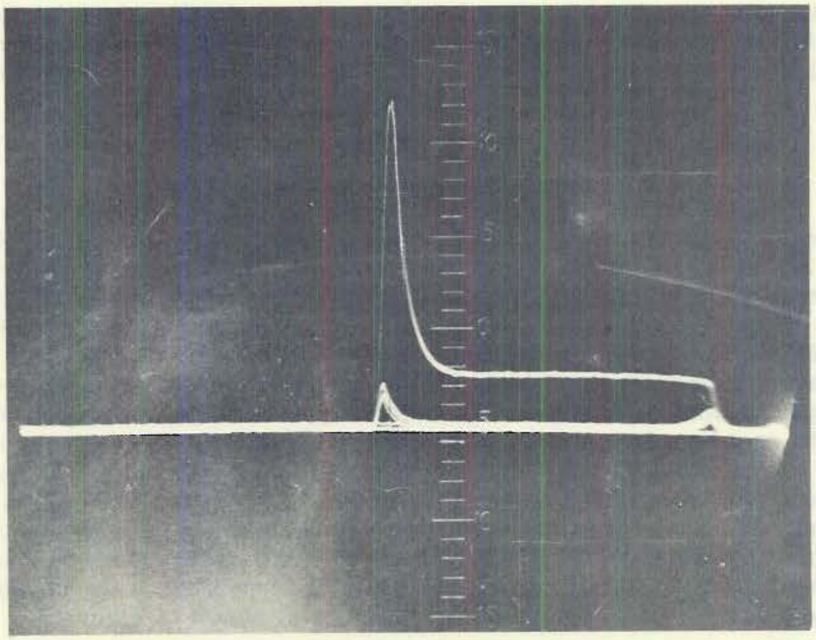

Figure 7 - Output current waveform obtained with early model Haeff Memory Tube. Writing speed 0.0152 inches per microsecond

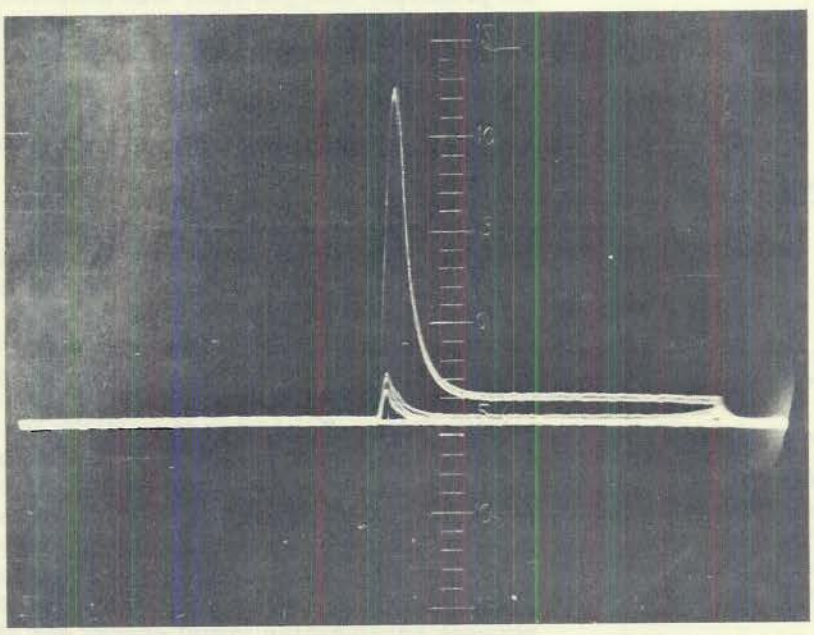

Figure 8 - Same as Figure 7 except writing speed 0.00715 inches per microsecond

base line, since the erasure pulse was delayed in phase, and the output during hold gun "flooding" is not shown. The similarity of the output current on the first scan after erasure to the curves of Figure 6 is apparent, including the qualitative dependence on writing speed.

PART III

SPOT CHARGING WITH REDISTRIBUTION

In this case it is necessary to consider the effect of those secondary electrons which return with low energy to the region around the spot. Since the secondary emission ratio is close to zero for low energies, most of these electrons "stick" where they land and depress the effective potential of this region. In the absence of these redistributed electrons, the dielectric surface near the positively charged spot would be at a positive potential with respect to ground, the potential varying inversely with distance from the spot. Thus we might expect a tendency for the returning secondaries to pile up in the immediate vicinity of the spot boundary and for their number to fall off with distance in the same general way as the potential falls off in their absence. At any rate, it is quite certain experimentally that most of the returning secondaries are deposited within two or three spot diameters of the center of the spot, although evidence of their presence is found out to ten or more spot diameters. In order that additional secondaries may arrive at any point, the resultant potential of that point must still be positive with respect to the collector. A qualitative sketch of these potential distributions is shown in Figure 9.

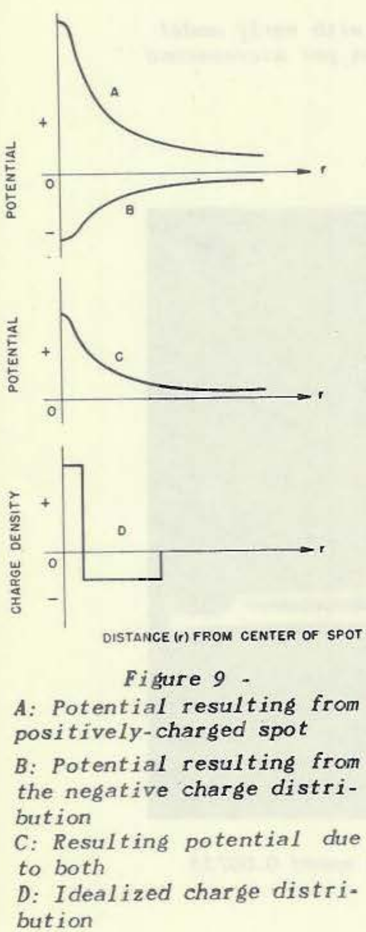

Figure 9 -
A: Potential resulting from positively-charged spot
B: Potential resulting from the negative charge distribution
C: Resulting potential due to both
D: Idealized charge distribution

As an approximation, this rather complex change distribution may conveniently be handled by introducing the idealizing concept of an equivalent constant-potential region of negative charge surrounding the spot. In what follows, this region of negative charge will be designated (by subscripts usually) as Region Two (2), with Region One (1) designating the positively charged spot, also assumed at constant potential. Thus the actual potential of any point of the screen may be written as some fraction of the ideal (positive) potential of the spot V_1 plus some fraction of the ideal (negative) potential of Region Two, the exact fractions depending on the distance of the point from the center of the spot and the size of the spot.

The paths of some typical secondary electrons may be imagined as sketched in Figure 10. Those secondaries with the lowest initial energy fall back into Region One before they have climbed very high on the potential hill surrounding the spot. Those electrons with higher initial energy attain greater heights before being forced to turn back and thus find themselves outside the boundaries of the spot (in Region Two) when they strike the screen. The very highest energy group is capable of reaching the top of the potential hill and striking the collector. Now the Z-directed initial energy required of a secondary electron to permit it to land at a given point depends not only on the location of the point but also on the initial direction of emission. Those electrons emitted almost normal to the surface may possess considerable initial energy and still return to the spot, but those electrons making a large angle with the normal may land in Region Two with much smaller amounts of Z-directed initial energy.

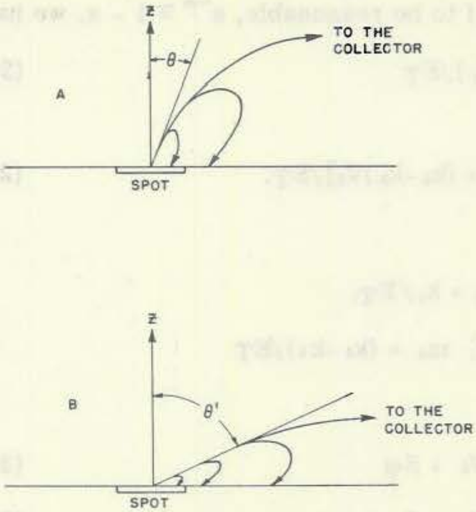

Figure 10 - Secondary electron paths for two different angles of emission

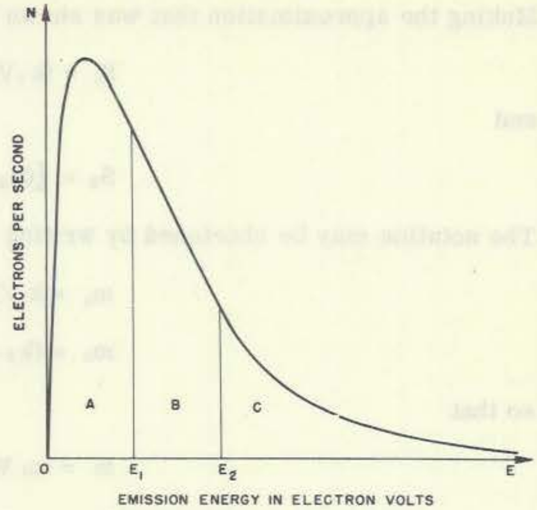

Figure 11 - Energy distribution curve showing:
A: Those secondaries returning to Region One
B: Those secondaries returning to Region Two
C: Those secondaries reaching the collector

An energy distribution curve as in Figure 11 may be drawn for a given initial direction angle of emission and divided into three parts as shown corresponding to the three groups of secondaries. The values of E_1 and E_2 setting the limits of these parts may be expressed in terms of the potentials of Regions One and Two, but may be expected to vary with θ, the direction angle of emission.

The argument of Part I must now be modified, since there are two regions of interest at different potentials charging at different rates. Hence there are two differential equations:

$$I_1 = \delta I_0 - I_0 - S_1 \delta I_0 = C_1 \frac{dV_1}{dt} \tag{24}$$

$$I_2 = -S_2 \delta I_0 = C_2 \frac{dV_2}{dt} . \tag{25}$$

These equations are not independent, however, since the fractional number of secondaries which return to Regions One (S_1) and Two (S_2) depends on the potential of both regions. This dependence is linear but varies from point to point throughout both regions. Hence, it is necessary to average over these regions by defining some new parameters dependent on the geometry (chiefly spot size), and the angular distribution characteristic of the secondary emitting material. Thus, k_1, k_2, k_3 and k_4 will be defined such that, when averaged over the respective regions and all direction angles of emission, secondary electrons with initial kinetic energy less than $k_1 V_1 + k_3 V_2$ return to Region One, while secondary electrons with initial kinetic energy between $k_1 V_1 + k_3 V_2$ and $k_2 V_1 + k_4 V_2$ return to Region Two. Then, by an argument similar to that of part I,

$$S_1 = 1 - e^{-(k_1 V_1 + k_3 V_2)/E_T} \tag{26}$$

and

$$S_2 = e^{-(k_1 V_1 + k_3 V_2)/E_T} - e^{-(k_2 V_1 + k_4 V_2)/E_T} . \tag{27}$$

Making the approximation that was shown in Part I to be reasonable, $e^{-x} \cong 1 - x$, we have

$$S_1 = (k_1 V_1 + k_3 V_2)/E_T \quad (28)$$

and

$$S_2 = [(k_2 - k_1)V_1 + (k_4 - k_3)V_2]/E_T. \quad (29)$$

The notation may be shortened by writing

$$m_1 = k_1/E_T, \quad m_3 = k_3/E_T,$$

$$m_2 = (k_2 - k_1)/E_T, \quad m_4 = (k_4 - k_3)/E_T$$

so that

$$S_1 = m_1 V_1 + m_3 V_2 + S_{01} \quad (30)$$

$$S_2 = m_2 V_1 + m_4 V_2 + S_{02}. \quad (31)$$

Both S_1 and S_2 have been increased by the constant terms S_{01} and S_{02} in order to take account of residual fields which may penetrate in some cases to the region around the spot and may cause the return of some secondary electrons to the screen even when the screen bears no positive charge. The restrictions on S mentioned in Part I apply here also in the form $0 \leq S_1 + S_2 \leq 1$, limiting the total output current to $(\delta - 1)I_0$ and $-I_0$ respectively.

The differential equations now become

$$C_1 \frac{dV_1}{dt} = (\delta - 1)I_0 - \delta I_0(S_{01} + m_1 V_1 + m_3 V_2) \quad (32)$$

$$C_2 \frac{dV_2}{dt} = -\delta I_0(S_{02} + m_2 V_1 + m_4 V_2), \quad (33)$$

which may be abbreviated

$$\frac{dV_1}{dt} + A_1 V_1 = B_1 + D_1 V_2 \quad (34)$$

$$\frac{dV_2}{dt} + A_2 V_2 = B_2 + D_2 V_1, \quad (35)$$

where

$$A_1 = m_1 \delta I_0 / C_1 \quad (36)$$

$$A_2 = m_4 \delta I_0 / C_2 \quad (37)$$

$$B_1 = [(\delta - 1)I_0 - S_{01}\, \delta I_0] / C_1 \quad (38)$$

$$B_2 = -S_{02}\, \delta I_0 / C_2 \quad (39)$$

$$D_1 = -m_3 \delta I_0 / C_1 \quad (40)$$

$$D_2 = -m_2 \delta I_0 / C_2. \quad (41)$$

Equations (34) and (35) may be solved simultaneously to obtain the solutions

$$V_1 = X_1 e^{M_1 t} + Y_1 e^{M_2 t} + W_1 \tag{42}$$

$$V_2 = X_2 e^{M_1 t} + Y_2 e^{M_2 t} + W_2, \tag{43}$$

where M_1 and M_2 are given by the two solutions of the equation

$$M^2 + (A_1 + A_2)M + A_1A_2 - D_1D_2 = 0 \tag{44}$$

and

$$W_1 = \frac{A_2B_1 + D_1B_2}{A_1A_2 - D_1D_2} \tag{45}$$

$$W_2 = \frac{A_1B_2 + B_1D_2}{A_1A_2 - D_1D_2}. \tag{46}$$

Solving equation (44) gives

$$M = \frac{-1}{2}\left[A_1 + A_2 \pm \sqrt{(A_1+A_2)^2 - 4(A_1A_2-D_1D_2)}\right] \tag{47}$$

$$= \frac{-\delta I_0}{2}\left[\frac{m_1}{C_1} + \frac{m_4}{C_2} \pm \sqrt{\left(\frac{m_1}{C_1} + \frac{m_4}{C_2}\right)^2 - 4\left(\frac{m_1m_4 - m_2m_3}{C_1C_2}\right)}\right] \tag{48}$$

From the differential equations and their solutions, we also obtain

$$\left.\begin{aligned} (M_1+A_1)X_1 &= D_1X_2, \quad (M_1+A_2)X_2 = D_2X_1 \\ (M_2+A_1)Y_1 &= D_1Y_2, \quad (M_2+A_2)Y_2 = D_2Y_1 \end{aligned}\right\} \tag{49}$$

$$A_1W_1 = B_1 + D_1W_2, \quad A_2W_2 = B_2 + D_2W_1.$$

From the initial conditions that $V_1 = V_{i1}$ and $V_2 = V_{i2}$ when $t = 0$, we have

$$\begin{aligned} X_1 + Y_1 + W_1 &= V_{i1} \\ X_2 + Y_2 + W_2 &= V_{i2}. \end{aligned} \tag{50}$$

Combining equations (49) and (50), we find that:

$$X_1 = \frac{(M_2+A_1)(W_1-V_{i1}) - D_1(W_2-V_{i2})}{M_1 - M_2} \tag{51}$$

$$X_2 = \frac{(M_2+A_2)(W_2-V_{i2}) - D_2(W_1-V_{i1})}{M_1 - M_2}. \tag{52}$$

It will be noted that W_1, W_2, X_1, X_2, Y_1 and Y_2 are all independent of beam current but that M_1 and M_2 are directly proportional to both beam current and secondary emission ratio. Since W_1 and W_2 represent the final potentials approached by the surface, they will hereafter be referred to as the equilibrium potentials V_{e1} and V_{e2}, respectively. We will designate by M_2 the value of M corresponding to the use of the positive sign in equation (48) and by M_1, that due to the negative sign. Hence, M_2 will represent the sum of two positive terms and M_1 their difference. The reciprocals of M_1 and M_2, designated by T_1 and T_2, respectively, will then be long and short time-constants respectively.

The output current may now be obtained from

$$I = C_1 \frac{dV_1}{dt} + C_2 \frac{dV_2}{dt} \tag{53}$$

as

$$I = C_1M_1X_1 e^{M_1t} + C_1M_2Y_1 e^{M_2t} + C_2M_1X_2 e^{M_1t} + C_2M_2Y_2 e^{M_2t} \tag{54}$$

and, combining terms,

$$I = M_1(C_1X_1 + C_2X_2) e^{M_1t} + M_2(C_1Y_1 + C_2Y_2) e^{M_2t}. \tag{55}$$

The functional dependence on beam current may be brought out more clearly by writing

$$M_1 = -\delta I_0 N_1, \quad M_2 = -\delta I_0 N_2$$

where

$$N_1 = \frac{1}{2}\left[\frac{m_1}{C_1} + \frac{m_4}{C_2} - \sqrt{\left(\frac{m_1}{C_1} + \frac{m_4}{C_2}\right)^2 - 4\left(\frac{m_1m_4 - m_2m_3}{C_1C_2}\right)}\right] \tag{56}$$

and

$$N_2 = \frac{1}{2}\left[\frac{m_1}{C_1} + \frac{m_4}{C_2} + \sqrt{\left(\frac{m_1}{C_1} + \frac{m_4}{C_2}\right)^2 - 4\left(\frac{m_1m_4 - m_2m_3}{C_1C_2}\right)}\right] \tag{57}$$

are independent of beam current or secondary emission ratio but depend on spot size and other characteristics of the tube. The output current, with this substitution, becomes

$$I = \delta I_0 \left[-N_1(C_1X_1 + C_2X_2) e^{-\delta I_0 N_1 t} - N_2(C_1Y_1 + C_2Y_2) e^{-\delta I_0 N_2 t}\right]. \tag{58}$$

The dependence of the output current on the initial potentials is emphasized by using the relations between X_1, X_2, Y_1, and Y_2 to obtain

$$\frac{I}{\delta I_0} = [H_1(V_{e1}-V_{i1}) + H_2(V_{e2}-V_{i2})] e^{-\delta I_0 N_1 t} + [H_3(V_{e1}-V_{i1}) + H_4(V_{e2}-V_{i2})] e^{-\delta I_0 N_2 t} \tag{59}$$

where

$$H_1 = \frac{N_1}{N_1 - N_2}(m_1 - C_1N_2)\left(1 + \frac{C_2N_1}{m_3} - \frac{C_2m_1}{C_1m_3}\right) \qquad H_3 = \frac{-N_2}{N_1 - N_2}(m_1 - C_1N_1)\left(1 + \frac{C_2N_2}{m_3} - \frac{C_2m_1}{C_1m_3}\right)$$

$$H_2 = \frac{N_1}{N_1 - N_2}\left(C_2N_1 - \frac{C_2m_1}{C_1} + m_3\right) \qquad H_4 = \frac{-N_2}{N_1 - N_2}\left(C_2N_2 - \frac{C_2m_1}{C_1} + m_3\right). \tag{60}$$

It was previously pointed out that M_2 would be expected to be larger than M_1 and hence N_2 larger than N_1. This is borne out experimentally; the factor N_2/N_1 is large. The output current thus turns out to be the sum of a small-amplitude, long time-constant component; and a large-amplitude, short time-constant component. The latter component is of positive polarity experimentally if both initial potentials are nearly zero, and may be interpreted as chiefly representing the net positive current to the spot which, having small capacitance to ground because of its small size, charges rapidly to its equilibrium potential. The former component may be interpreted as the redistributed-electron current, which continues to charge the relatively large capacitance of the region about the spot for a long time. Experimentally, this longer time-constant does not seem to remain constant with time but approaches a limiting value which is independent of beam current after hundreds of microseconds. Apparently the initial assumption that Region Two remained fixed in area indefinitely is not valid after a sufficient time, as might have been expected, but that on the contrary, the higher-energy secondaries continue to land on the border, so that the boundary slowly spreads out.

The general behavior of the output is experimentally as predicted, however, as shown by Figures 12 through 15. Figure 12 is an oscilloscope photograph of the output current versus time and clearly shows the two components referred to above. The experimental technique was to pulse the primary beam on for several 43-microsecond intervals instead of for one longer interval. Thus, the output during several hundred microseconds is shown in the figure with the positive peak indicating the start of the process. Figures 13 and 14 show the amplitude of positive and negative peaks of such curves as determined experimentally, plotted versus beam current over nearly a hundred-to-one range. Figure 15 is a plot of the reciprocal of the time constant of the positive component over the same range in beam current. The time constant of the negative component is not plotted; there are experimental difficulties associated with measuring accurately this very low rate of change of current, and, as mentioned above, the time constant varies with time. The spot diameter for Figures 13 through 15 was 0.6 cm, representing a beam which was purposely defocused in order to stretch out the positive component of the output in time to permit more accurate measurement. As shown by equations 56 and 57, the N_1 and N_2 factors vary inversely with the capacitance coefficients. Thus, increasing C_1 and C_2 by increasing the spot size reduces N_1 and N_2 and therefore increases the corresponding time constants. Although this change in spot size might be expected to change the m factors also, the experimental result indicates that their relation to spot size is less than a direct proportionality. Further experimental work will be required to establish this relationship exactly.

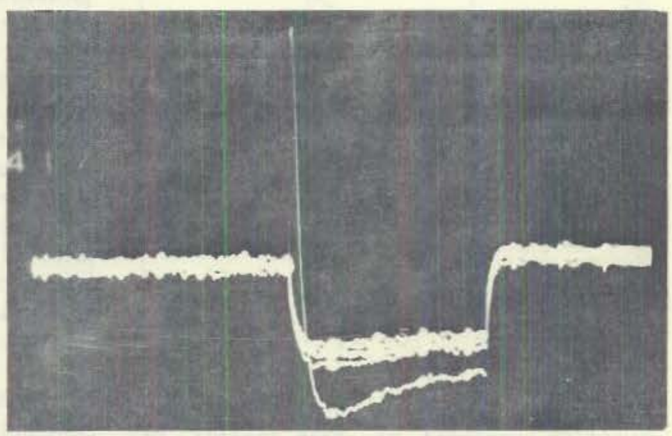

Figure 12 - Photograph of output current from a stationary spot with redistribution. Commercial 5JP5 cathode-ray tube. Beam current 0.130 microamperes

PART IV

SCANNING WITH REDISTRIBUTION

The general procedure of Part II may now be repeated using the values for the potentials obtained in Part III, but it must be recognized that this formal process ignores some fundamental physical facts of redistribution. The secondary electrons returning to Region Two

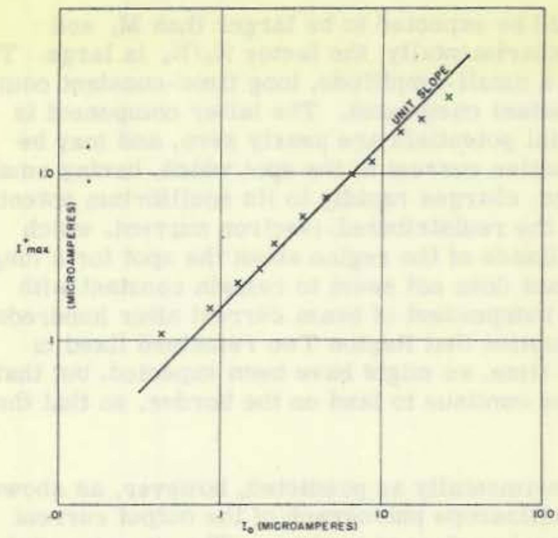

Figure 13 - Positive peak current vs. beam current. Stationary spot with redistribution. Crosses show experimental points

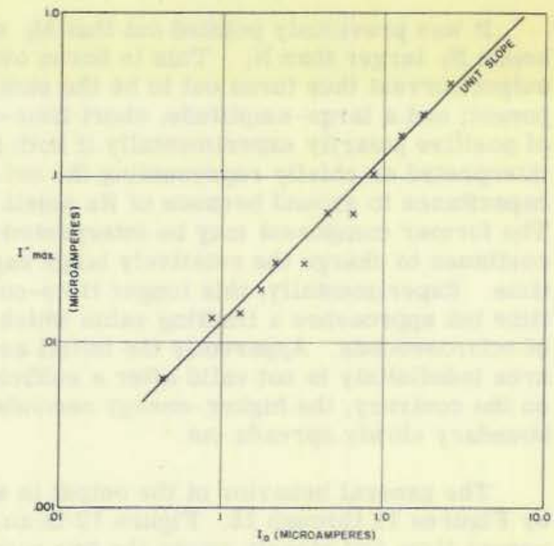

Figure 14 - Negative peak current vs. beam current. Stationary spot with redistribution. Crosses show experimental points

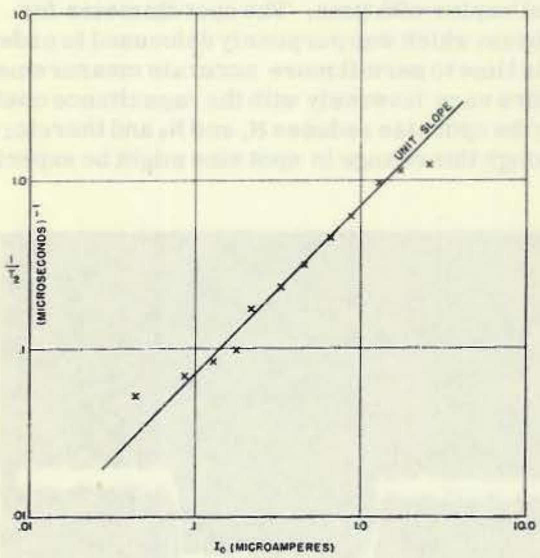

Figure 15 - Reciprocal of time constant of positive component vs. beam current. Stationary spot with redistribution. Crosses show experimental points

fall in part ahead and in part behind the scanning beam as well as on each side of the line of scan. Thus, when the beam reaches any particular point, it finds an "initial" potential which is more negative than it was before the beam approached its vicinity and, after the beam has passed by, the point again goes negative in potential since it is again in a Region Two of nearby points. Furthermore, points off the line of scan are bombarded by secondary electrons during the time that the scanning beam moves several times its own width, in contrast to the no-redistribution case of Part II in which the steady-state current and potential were reached in the time required for the beam to move just once its own width. Also, the division of secondaries between the different regions of the screen may be affected by the potential of the line of scan, both ahead of and behind the spot.

These complications might be taken into account, at least approximately, by considering four areas or regions to move along with the moving beam, as shown in Figure 16. Region One as before would designate the equivalent area struck by the primary beam; Region Two,

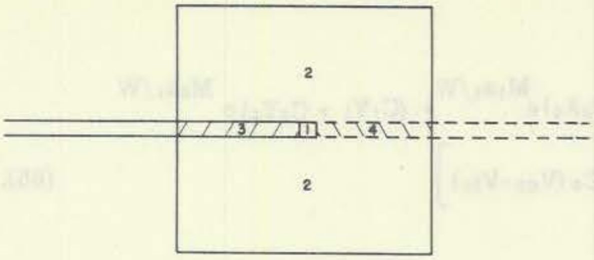

Figure 16 - Instantaneous position of moving spot showing four idealized regions of charge

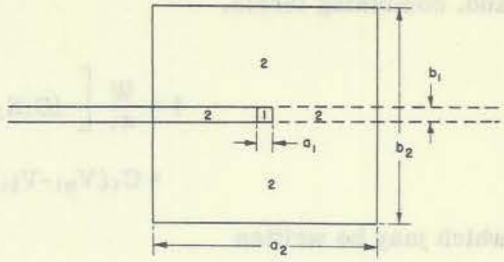

Figure 17 - Instantaneous position of moving spot showing idealized Regions One and Two

the equivalent area off the line of scan which is struck by returning secondaries from Region One; Region Three, the area of the line of scan behind the spot receiving secondaries from Region One; and, finally, Region Four, the area of the line of scan ahead of the spot receiving secondaries from Region One. After the resulting differential equations for the potentials of these four regions have been derived and solved, the steady-state current might be found by successive integrations over distances equal to the spot width, using for the initial potentials at each integration the values found by the previous integration.

However, this process is laborious and the necessary expressions so unwieldy that a simpler if less accurate analysis will be given here. The final establishment of the limits of validity of the results can only (as in any case) be obtained by resorting to experiment.

We proceed then to find the steady-state output current by integration over the areas shown in Figure 17. As in Part II, the current to Region One is

$$I_1 = \int_0^{a_1} \frac{C_1}{a_1} \frac{dV_1}{dt} dx = \frac{WC_1}{a_1} \left[V_1\left(t = \frac{a_1}{W}\right) - V_{i1} \right]. \tag{61}$$

As an approximation, the current to Region Two is a_2/a_1 times the current to an area b_2 in height and a_1 in width, or

$$I_2 = \frac{a_2}{a_1} \int_0^{a_1} \frac{C_2}{a_2} \frac{dV_2}{dt} dx = \frac{WC_2}{a_1} \left[V_2\left(t = \frac{a_1}{W}\right) - V_{i2} \right]. \tag{62}$$

The total output current then is

$$I = I_1 + I_2 \tag{63}$$

and, introducing the expressions for the potentials from Part III, we have

$$I = \frac{W}{a_1} \Big[C_1X_1e^{M_1a_1/W} + C_1Y_1e^{M_2a_1/W} + C_1(V_{e1} - V_{i1})$$

$$+ C_2X_2e^{M_1a_1/W} + C_2Y_2e^{M_2a_1/W} + C_2(V_{e2} - V_{i2}) \Big] \tag{64}$$

and, combining terms,

$$I = \frac{W}{a_1}\left[(C_1X_1 + C_2X_2)e^{M_1a_1/W} + (C_1Y_1 + C_2Y_2)e^{M_2a_1/W} + C_1(V_{e1}-V_{i1}) + C_2(V_{e2}-V_{i2}) \right] \tag{65}$$

which may be written

$$I = \frac{W}{a_1}\left\{\left[K_1(V_{e1}-V_{i1}) + K_2(V_{e2}-V_{i2})\right]e^{-\delta I_0N_1a_1/W} - \left[K_3(V_{e1}-V_{i1}) + K_4(V_{e2}-V_{i2})\right]e^{-\delta I_0N_2a_1/W} + C_1(V_{e1}-V_{i1}) + C_2(V_{e2}-V_{i2})\right\} \tag{66}$$

where

$$\left.\begin{aligned}
K_1 &= \frac{-H_1}{N_1} = \frac{C_1N_2-m_1}{N_1-N_2}\left(1 + \frac{C_2N_1}{m_3} - \frac{C_2m_1}{C_1m_3}\right)\\
K_2 &= \frac{-H_2}{N_1} = \frac{-m_3}{N_1-N_2}\left(1 + \frac{C_2N_1}{m_3} - \frac{C_2m_1}{C_1m_3}\right)\\
K_3 &= \frac{-H_3}{N_2} = \frac{C_1N_1-m_1}{N_1-N_2}\left(1 + \frac{C_2N_2}{m_3} - \frac{C_2m_1}{C_1m_3}\right)\\
K_4 &= \frac{-H_4}{N_2} = \frac{-m_3}{N_1-N_2}\left(1 + \frac{C_2N_2}{m_3} - \frac{C_2m_1}{C_1m_3}\right)
\end{aligned}\right\} \tag{67}$$

From these expressions, the output current is zero for beam current zero and approaches a constant value for very high beam current. If we assume as before that N_1 is small compared to N_2, then the first exponential in equation (66) is close to unity for at least all values of the parameters for which the second exponential differs appreciably from zero. Hence, the approximation

$$e^{-\delta I_0N_1a_1/W} \cong 1 - \frac{\delta I_0N_1a_1}{W}$$

may be used, giving

$$I = \frac{W}{a_1}\left[(K_1 + C_1)(V_{e1}-V_{i1}) + (K_2 + C_2)(V_{e2}-V_{i2})\right]\left(1 - e^{-\delta I_0N_2a_1/W}\right) - \left[K_1(V_{e1}-V_{i1}) + K_2(V_{e2}-V_{i2})\right]\delta I_0N_1 \tag{68}$$

where the relations

$$K_1 + C_1 = K_3 \tag{69}$$

$$K_2 + C_2 = K_4 \tag{70}$$

have been used. From the defining equations (67), K_1 is positive and K_2 negative if all three of the following plausible conditions are satisfied:

$$(1) \quad N_2 > N_1 \tag{71}$$

$$(2) \quad N_2 > m_1/C_1 \tag{72}$$

$$(3) \quad \frac{C_2 m_1}{C_1 m_3} > 1 + \frac{C_2 N_1}{m_3}\,. \tag{73}$$

The equilibrium potentials V_{e1} and V_{e2} are positive and negative respectively, so that if both initial potentials are zero or positive, the term proportional to primary beam current is negative while the first term is positive if

$$|K_2| > C_2$$

or, more generally, if

$$(K_1 + C_1)\,(V_{e1}-V_{i1}) > (K_2 + C_2)\,(V_{e2}-V_{i2})\,.$$

For easy comparison with experiment, equation (68) may be written in the abbreviated form

$$I = \alpha\beta\left(1-e^{-I_0/\alpha}\right) - \gamma I_0 \tag{74}$$

in which

$$\alpha = \frac{W}{\delta a_1 N_2}$$

$$\beta = \delta N_2\left[(K_1 + C_1)\,(V_{e1}-V_{i1}) + (K_2 + C_2)\,(V_{e2}-V_{i2})\right]$$

$$\gamma = \delta N_1\left[K_1(V_{e1}-V_{i1}) + K_2(V_{e2}-V_{i2})\right]. \tag{75}$$

Equation (74) is plotted in Figure 18 as a function of beam current using experimental values for α, β and γ. Secondary emission ratio was 3.76 for P-5 phosphor operating at 1400 volts accelerating potential. Writing speed was 0.20 inches per microsecond with a sharply focused spot. Experimental points are shown by crosses in the figure. The linear dependence of α upon the writing speed has been checked by locating the points at which the output current is zero in the steady state. The beam current at these points turns out to be directly proportional to the writing speed, other parameters being held constant. For the three writing speeds 0.0247, 0.0817, and 0.200 inches per microsecond, the proportionality checked to within one percent. The probable error of the experimental points in general, however, is no better than ± 5 percent, due principally to variations in primary beam current.

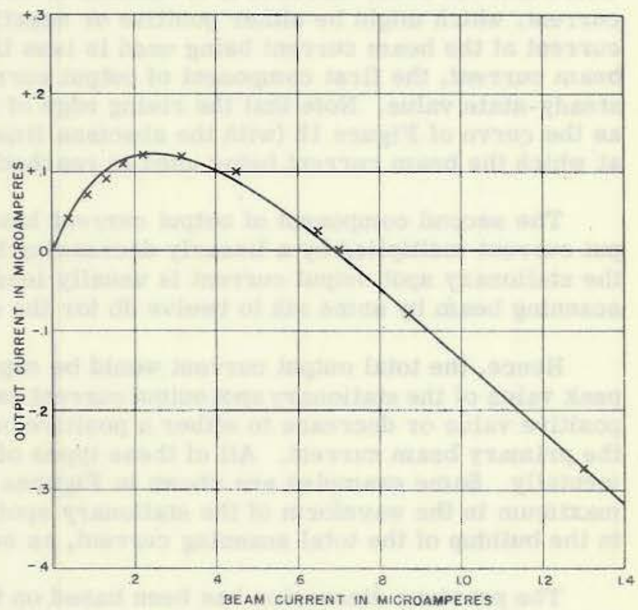

Figure 18 - Steady-state output current vs. beam current for scanning beam with redistribution. Writing speed 0.20 inches per microsecond. Crosses show experimental points. Curve is plot of equation

$$I = 0.325\left(1 - e^{-I_0/0.190}\right) - 0.460\, I_0$$

The transient current which flows when the primary beam current is first switched on (by a voltage step function on the control grid of the cathode-ray tube, say) may be obtained by the method used in the similar case in Part II with a similar result. The output current as a function of time is the sum of two components; one having the form of the steady-state current just derived but with a_1/W replaced by t and the other being the stationary spot current multiplied by the linearly decreasing factor $(1-Wt/a_1)$. Thus

$$I = \frac{W}{a_1}\left[(C_1X_1 + C_2X_2)e^{M_1t} + (C_1Y_1 + C_2Y_2)e^{M_2t} + C_1(V_{e1}-V_{i1}) + C_2(V_{e2}-V_{i2})\right] + \left(1-\frac{Wt}{a_1}\right)\left[M_1(C_1X_1 + C_2X_2)e^{M_1t} + M_2(C_1Y_1 + C_2Y_2)e^{M_2t}\right]. \quad (76)$$

Considering only the first component, as t goes through its possible values from zero to a_1/W, the first component of output current takes on the same values as the steady-state output current does when the primary beam current goes through its possible values from zero to the value being used. Thus, if the steady-state output current at the beam current being used is less positive than it would be at a lower beam current, corresponding to operation to the right of the maximum in Figure 18, the first component of output current would start at zero, increase to a maximum, and then decrease to the final steady-state current, which might be either positive or negative. If, however, the steady-state output current at the beam current being used is less than the maximum which occurs at a larger beam current, the first component of output current would increase monotonically to its steady-state value. Note that the rising edge of the waveform would be of the same shape as the curve of Figure 18 (with the abscissa time instead of beam current) up to the point at which the beam current being used is reached.

The second component of output current has the waveform of the stationary spot output current multiplied by a linearly decreasing factor. In our experience, the peak of the stationary spot output current is usually less than the steady-state output with a fast scanning beam by some six to twelve db for the same beam current.

Hence, the total output current would be expected from equation (76) to begin at the peak value of the stationary spot output current and then either increase gradually to its final positive value or decrease to either a positive or negative steady-state value depending on the primary beam current. All of these types of transients have been observed experimentally. Some examples are shown in Figures 19 through 22. Because of the negative maximum in the waveform of the stationary spot output current, a dip is sometimes seen in the buildup of the total scanning current, as seen particularly in Figure 20.

The previous discussion has been based on the application of an ideal switch to turn the primary beam current on and off. In practice, the leading edge of the pulsed signal applied to the control grid of the cathode-ray tube usually approaches this ideal fairly closely, but the trailing edge is usually not quite so good. This may give rise to an effect at the end of the pulse similar to the transient at the beginning, although occurring in much less time and sometimes obscured by the finite response time of the output amplifier. As the primary beam current decreases toward zero, the output current goes through its normal variation which may actually involve an increase in output current.

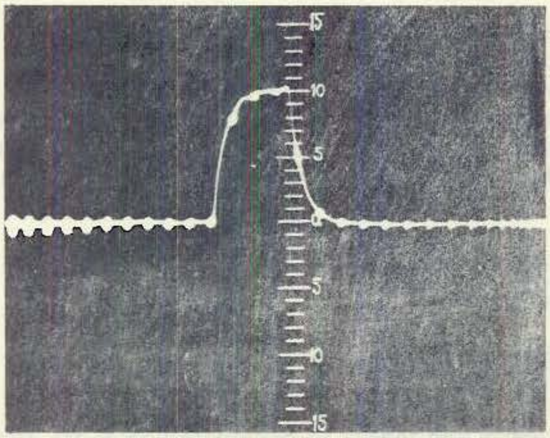

Figure 19 - Photograph of transient output current obtained with commercial 5JP5 cathode-ray tube. Writing speed 0.150 inches per microsecond. Beam current 0.130 microamperes, two-microsecond markers

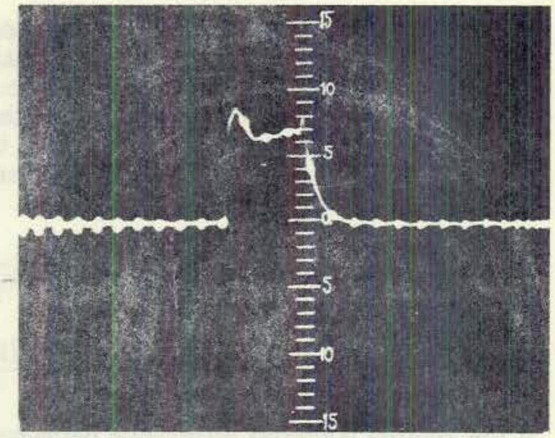

Figure 20 - Same as Figure 19 except beam current 0.650 microamperes

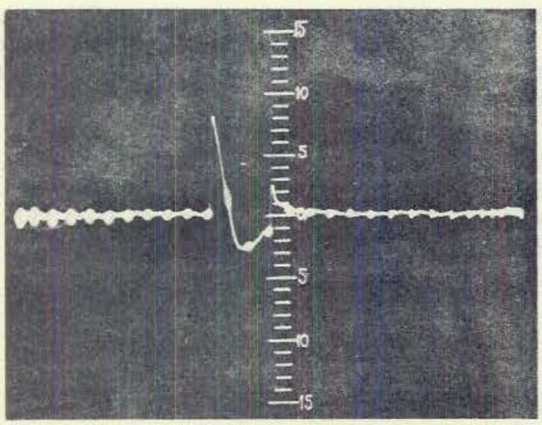

Figure 21 - Same as Figure 19 except beam current 0.780 microamperes

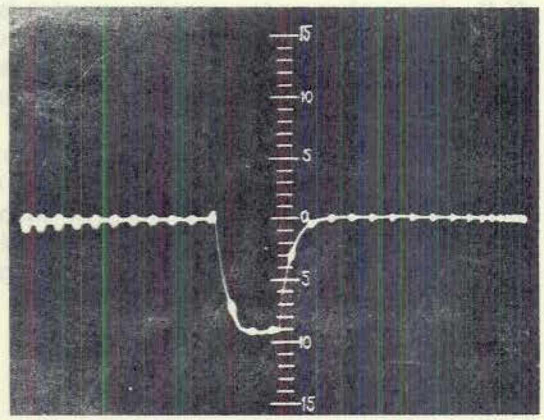

Figure 22 - Same as Figure 19 except beam current 1.30 microamperes

It will be observed in Figures 19 through 22 that the actual distance on the face of the cathode-ray tube required for the output current to reach a constant value is many times a spot diameter. This distance is really a measure of the extent of Region Two along the line of scan which was neglected in this approximate analysis. It appears, however, from the preceding qualitative discussion that the derived equations may satisfactorily describe the observed phenomena if the experimental value of the distance a_1 is used in the formulas. This distance, fortunately, appears to be at least approximately independent of beam current or writing speed in the range so far investigated and proved useful. No experimental information is yet available on its variation with spot size or other parameters.

APPLICATIONS

The theory so far developed may be extended to cover various interesting special cases, although the details will not be given here. Thus the effect of intensity modulation by an ideal square pulse on the output steady-state current has already been indicated. Modulation by a continuously varying voltage on the control grid or by deflection of the beam may be handled by point-by-point computations if the period of the modulation is long compared to the time required for the beam to move its own width. Variation of the voltage between target and collector has the effect of simultaneous variation of the factors S_{01} and S_{02} which influence the equilibrium potentials, since equations (45) and (46) when expanded become:

$$V_{e1} = \frac{m_4(1-1/\delta - S_{01}) + m_3 S_{02}}{m_1 m_4 - m_2 m_3} \qquad (77)$$

$$V_{e2} = \frac{-m_2(1-1/\delta - S_{01}) - m_1 S_{02}}{m_1 m_4 - m_2 m_3}. \qquad (78)$$

If the applied potential difference between collector and target is designated as $V_C(t)$, then the linear approximation previously used gives

$$S_{01} = S'_{01} + (m_1 + m_3)\, V_C\,(t) \qquad (79)$$

$$S_{02} = S'_{02} + (m_2 + m_4)\, V_C\,(t). \qquad (80)$$

If V_C does not vary too rapidly, a point-by-point computation is again possible. Otherwise it is necessary to find the particular solutions of the differential equations for the surface potentials corresponding to the applied function $V_C(t)$ and add these to the solutions already obtained in carrying out the subsequent integration.

Much experimental work remains to be done to check the validity of the theory presented here. In particular, the effect of variation in initial potentials needs quantitative investigation in view of the complex phenomena (pointed out at the beginning of Part IV) which have been neglected in the simplified theory. Qualitatively, however, the experiments which have so far been performed appear to confirm the simple theory for the range of parameters investigated.

ACKNOWLEDGMENT

The experimental results in this report were obtained by Mr. W. A. White and Mr. J. E. Scobey of the Naval Research Laboratory.

* * *

NAVY-DPPO PRNC. WASH., D.C.